

# LOAN DOCUMENT

PHOTOGRAPH THIS SHEET

AD-A956 006



DTIC ACCESSION NUMBER

LEVEL

LEVEL

INVENTORY

INVENTORY

TR-76-11

DOCUMENT IDENTIFICATION

Nov 1974

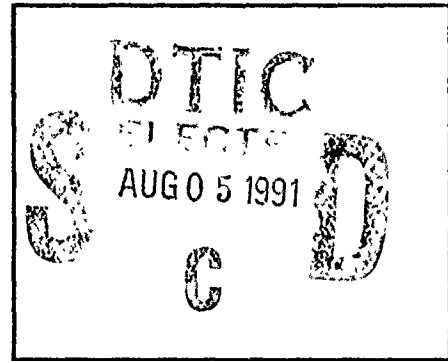
DISTRIBUTION STATEMENT A

Approved for public release;  
Distribution Unlimited

DISTRIBUTION STATEMENT

ACCESSION FOR	
NTIS	GRA&I
DTIC	TRAC
UNANNOUNCED	<input checked="" type="checkbox"/>
JUSTIFICATION	
BY <i>Poc R034 095</i>	
DISTRIBUTION/	
AVAILABILITY CODES	
DISTRIBUTION	AVAILABILITY AND/OR SPECIAL
A-1	

DISTRIBUTION STAMP



DATE ACCESSIONED

DATE RETURNED

DATE RETURNED

REGISTERED OR CERTIFIED NUMBER

REGISTERED OR CERTIFIED NUMBER

28 91 7 30 028  
91-06535

DATE RECEIVED IN DTIC

PHOTOGRAPH THIS SHEET AND RETURN TO DTIC-FDAC

H  
A  
N  
D  
L  
E  
  
W  
I  
T  
H  
  
C  
A  
R  
E

**AD-A956 006**



---

TECHNICAL REPORT NO. 76-11

ASYMPTOTIC SOLUTION OF SURFACE FIELD  
DUE TO A MAGNETIC DIPOLE ON A CYLINDER

S. W. Lee  
S. Safavi-Naini

Electromagnetics Laboratory Report No. 76-11

ASYMPTOTIC SOLUTION OF SURFACE FIELD  
DUE TO A MAGNETIC DIPOLE ON A CYLINDER

By

S. W. Lee  
S. Safavi-Naini

Technical Report

November 1976

Supported by  
Contract No. N00019-76-M-0622  
Department of the Navy  
Naval Air Systems Command  
Washington, D.C. 20361

Electromagnetics Laboratory  
Department of Electrical Engineering  
Engineering Experiment Station  
University of Illinois at Urbana-Champaign  
Urbana, Illinois 61801

## ABSTRACT

A simple, approximate expression for the surface magnetic field due to a magnetic dipole on a conducting circular cylinder is obtained. This solution is asymptotic for a large cylinder radius, and is uniformly valid everywhere on the cylindrical surface including the penumbra and the deep shadow. In the limit that the cylinder radius is infinite, it becomes identical to the known exact solution of a dipole on a conducting plane. For a surface ray propagating in parallel to the axis of the cylinder, the transverse surface magnetic field is found to vary asymptotically as  $(ks)^{-1/2}$ , where  $s$  is the distance from the source. This behavior is distinctively different from the  $(ks)^{-1}$  variation of the surface ray on a plane, and is explained in terms of the dependence of the surface curvature in the binormal direction of the ray. We apply our solution to the mutual coupling problem between two slots on a cylinder, and obtain results which are in excellent agreement with those calculated from the exact modal solution. A comparison of the present solution with two other asymptotic (GTD) solutions is also given.

## ACKNOWLEDGEMENT

The work reported here has been supported by the Department of the Navy, Naval Air Command under contract N00019-76-M-0622. The discussions with and suggestions by P. C. Bargeliotas, R. C. Hansen, A. Hessel, Y. Hwang, W. H. Kummer, R. Mitra, P. H. Pathak, and J. Willis were helpful. A part of the computer programming was done by P. Chang.

## TABLE OF CONTENTS

	Page
1. INTRODUCTION . . . . .	1
2. UI SOLUTION FOR THE SURFACE MAGNETIC FIELD . . . . .	3
3. COMPARISON WITH OSU SOLUTION . . . . .	9
4. COMPARISON WITH PINY SOLUTION. . . . .	12
5. APPLICATION: MUTUAL ADMITTANCE OF SLOTS . . . . .	20
6. DERIVATION OF UI SOLUTION. . . . .	27
7. CONCLUSION . . . . .	31
APPENDIX - FOCK FUNCTIONS. . . . .	32
REFERENCES . . . . .	37

## LIST OF ILLUSTRATIONS

Figure	Page
1. A surface ray from source point $Q'$ to observation point $Q$ on a cylinder of radius $R$ . . . . .	4
2. $H_\phi$ along a surface ray in $\theta = 0^\circ$ direction on a cylinder vs. the distance from the $\phi$ -directed magnetic dipole . . . . .	15
3. $H_\phi$ along a surface ray in $\theta = 45^\circ$ direction on a cylinder vs. the distance from the $\phi$ -directed magnetic dipole . . . . .	16
4. $H_\phi$ along a surface ray in $\theta = 90^\circ$ direction on a cylinder vs. the distance from the $\phi$ -directed magnetic dipole . . . . .	17
5. $H_\phi$ along a surface ray in $\theta = 90^\circ$ direction on a cylinder vs. the distance from the $\phi$ -directed magnetic dipole . . . . .	18
6. Surface magnetic field $ H_\phi $ on a cylinder with $kR = 9.5325$ due to a circumferential dipole ( $\vec{M} = \hat{\phi}$ ) calculated from (2.6). Values above 7.475 db are not shown . . . . .	19
7. Two identical circumferential slots on the surface of a cylinder. The figure shows the developed cylinder. . . . .	21
8. $Y_{12}$ on a cylinder as a function of the radius $R$ of the cylinder. $Y_{12}$ is normalized by $Y_{12}$ on a plane which is $5.37 \times 10^{-5} \exp(j53.55^\circ)$ mho . . . . .	26
9. A horizontal magnetic dipole on the surface of a perfectly conducting sphere. . . . .	28
10. Contours $\Gamma_1$ and $\Gamma_2$ on the complex $t$ (or $z$ ) plane. $\Gamma_1$ , for example, goes from $\infty$ to 0 along the line $\text{Arg } t = -2\pi/3$ and from 0 to $\infty$ along the real axis. . . . .	33

## LIST OF TABLES

Table	Page
I. $Y_{12}$ FOR $\phi_0 = 0$ (E-PLANE) . . . . .	23
II. $Y_{12}$ FOR $z_0 = 2''$ . . . . .	24
III. $Y_{12}$ FOR $z_0 = 0$ (H-PLANE) . . . . .	24

## 1. INTRODUCTION

This paper considers a high-frequency diffraction problem by a perfectly conducting cylinder as sketched in Fig. 1a. For a given magnetic dipole at  $Q'$  on the surface of the cylinder, the problem is to find the surface magnetic field (surface current density) everywhere when  $kR$  is large ( $R$  is the radius of the cylinder and  $k = 2\pi/\lambda$ ). The motivations for our study are the following two: (i) The solution of the cylinder problem constitutes a central step in calculating the mutual coupling between two slots on the surface of a cylinder [1]-[8]. (ii) More importantly, the cylinder problem is a so-called "canonical problem" in GTD [9]-[11]. Once its solution is known, it may be generalized, by following the recipe of the GTD, to give the asymptotic solution of the surface magnetic field on any convex, smooth, conducting surface.

The cylinder problem has an exact modal solution, which is in the form of an infinite series with each term containing an infinite integral [4], [5]. For a large  $kR$ , this solution is very slowly convergent and becomes less useful. Two asymptotic solutions exist in the literature: one given by Hwang, Kouyoumjian, and Pathak [5], [6] (hereafter referred to as the OSU solution), and the other by Chang, Felsen, Hessel and Shmoys [3], [4] (the PINY solution). Both are approximately deduced from the exact modal solution under the condition  $kR \rightarrow \infty$ . In the present paper, we offer a third asymptotic solution (the UI solution), which gives the surface magnetic field everywhere from the source point to the deep shadow in a single expression, and is based on a classical work by Fock in 1949 (Chapter 12 of [12]).

The organization of this paper is as follows. In Sections 2 through 4, the final form of the UI solution is stated and compared with those of OSU and PINY. In Section 5, the three asymptotic solutions are applied to the evaluation of the mutual admittance between two slots on a cylinder. Their

results are compared with those calculated from the exact modal solutions [2], [7], [8]. Section 6 describes the derivation of the UI solution. Finally, a conclusion is given in Section 7. Some formulas of Fock functions used in the text are listed in the Appendix.

## 2. UI SOLUTION FOR THE SURFACE MAGNETIC FIELD

At point  $Q'$  on the surface of the cylinder (Fig. 1a), there is a tangential magnetic dipole source described by a magnetic current density (for  $\exp +j\omega t$  time convention).

$$\vec{K}(\vec{r}) = \vec{M} \frac{1}{R} \delta(r - R) \delta(\phi) \delta(z) \quad (2.1)$$

where  $\vec{M}$  is the magnetic dipole moment ( $\vec{M} \cdot \hat{r} = 0$ ), and  $(r = R, \phi = 0, z = 0)$  are the cylindrical coordinates of  $Q'$ . The problem is to determine  $\vec{H}$  at another point  $Q = (R, \phi, z)$  on the surface under the assumption that  $kR$  is large.

First, let us introduce several parameters. According to GTD [9], [11], the dominant contribution of  $\vec{H}$  at  $Q$  is the field on the surface ray from  $Q'$  to  $Q$ . The surface ray is a geodesic on the conducting surface, and in the present case is a helical path (Figure 1). The arclength of the surface ray is

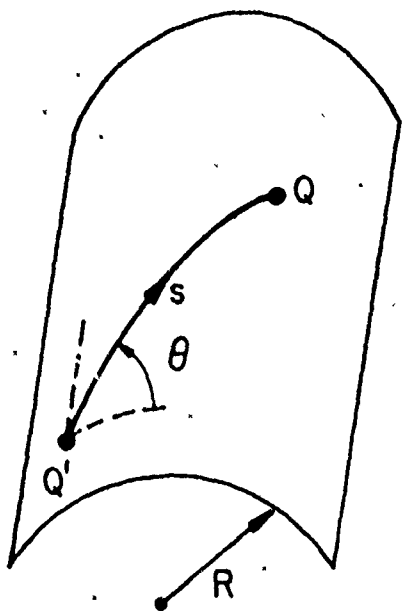
$$s = \sqrt{(R\phi)^2 + z^2} \quad (2.2)$$

The tangent, normal, and binormal of the surface ray are  $(\hat{t}', -\hat{n}', -\hat{b}')$  at  $Q'$ , and  $(\hat{t}, -\hat{n}, -\hat{b})$  at  $Q$ . Thus,  $(\hat{t}, \hat{n}, \hat{b})$  form a moving trihedron along a surface ray, pointing toward the longitudinal and two transverse directions. At any point on the surface ray, the curvature of the conducting surface is described by two parameters:

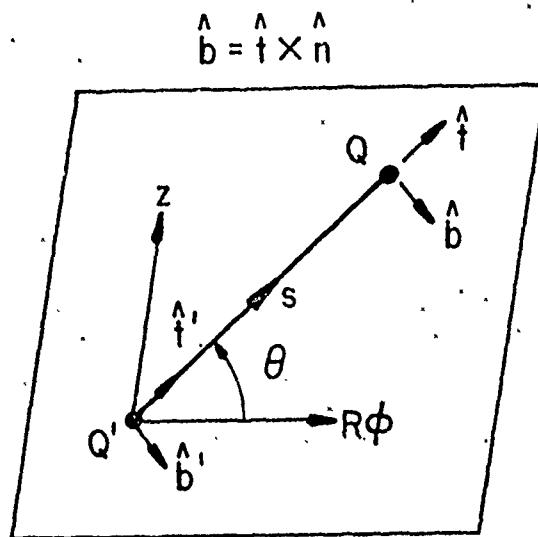
$R_t$  = the radius of curvature in the direction of  $\hat{t}$  (or that in the longitudinal direction of the surface ray), and

$R_b$  = the radius of curvature in the direction of  $\hat{b}$  (or that in the transverse direction of the surface ray).

On a convex surface, both  $R_t$  and  $R_b$  are nonnegative. For the present case of a conducting cylinder, one has



(a) 3-D view



(b) Developed cylinder

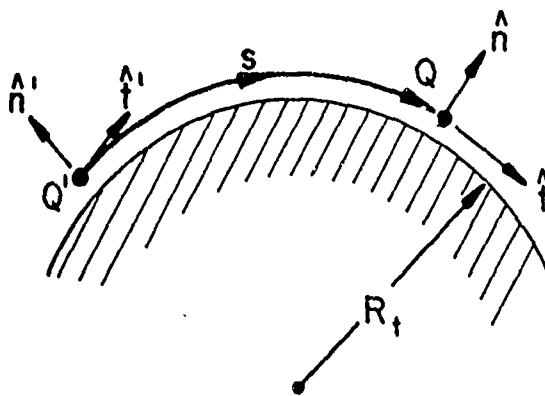
(c) Cut along  $\theta$ -direction

Figure 1. A surface ray from source point  $Q'$  to observation point  $Q$  on a cylinder of radius  $R$ .

$$R_t = \frac{R}{\cos^2 \theta}, \quad R_b = \frac{R}{\sin^2 \theta} \quad (2.3)$$

where  $\theta$  is measured from  $R\phi$ -axis in Fig. 1b, and takes a value between 0 and  $2\pi$ . The large parameter for our asymptotic expansion is

$$m = \left( \frac{1}{2} k R_t \right)^{1/3} \quad (2.4)$$

Thus, our solution is an approximate (not rigorous) asymptotic solution valid for  $m \rightarrow \infty$ , up to and including terms of  $O(m^{-3})$ . Furthermore, let us introduce a distance parameter

$$\xi = \frac{ms}{R_t} = \left( k/2R_t^2 \right)^{1/3} s = \frac{ks}{2m^2} \quad (2.5)$$

which is the arclength normalized by  $k$  and  $R_t$ . Note that  $\xi = 0$  defines the lit region ( $\theta = \pi/2$ ),  $\xi < 1$  defines the penumbra region, and  $\xi \gg 1$  defines the deep shadow. Our solution is uniformly valid for all  $\xi \geq 0$ .

Due to the point source in (2.1), our final asymptotic solution for the magnetic field on the surface is given by

$$\vec{H}(Q) = \vec{M} \cdot (\hat{b}'\hat{b}H_b + \hat{t}'\hat{t}H_t) + O(m^{-4}), \quad m \rightarrow \infty \quad (2.6a)$$

where the transverse component is

$$H_b(Q) \sim \left[ \left( 1 - \frac{j}{ks} \right) v(\xi) - \left( \frac{1}{ks} \right)^2 u(\xi) + j(\sqrt{2} k R_t)^{-2/3} v'(\xi) + j(\sqrt{2} k R_t)^{-2/3} (R_t/R_b) u'(\xi) \right] G(s), \quad (2.6b)$$

the longitudinal component is

$$H_t(Q) \sim \left( \frac{j}{ks} \right) \left[ v(\xi) + \left( 1 - \frac{2j}{ks} \right) u(\xi) + j(\sqrt{2} k R_t)^{-2/3} u'(\xi) \right] G(s), \quad (2.6c)$$

and the function  $G(s)$  is

$$G(s) = \frac{k^2 Y_0}{2\pi j} \frac{e^{-jks}}{ks} \quad (2.6d)$$

Here  $Y_0 = (\epsilon_0/\mu_0)^{1/2} = (120\pi)^{-1}$ ,  $v$  and  $u$  are defined in the Appendix, and  $v'$  is the derivative of  $v$ . We emphasize that (2.6) is an approximate solution. For one thing, we are not even able to show that (2.6a) contains all the terms up to  $O(m^{-3})$ , let alone other more subtle questions.

Let us consider several limiting cases of the UI solution given in (2.6). If the radius of the cylinder becomes infinite

$$kR \rightarrow \infty \quad (2.7)$$

the use of (A-12) through (A-16) in the Appendix in (2.6) leads to

$$H_b(Q) \sim \left[ 1 - \frac{j}{ks} - \left( \frac{1}{ks} \right)^2 \right] G(s), \quad kR \rightarrow \infty \quad (2.8a)$$

$$H_t(Q) \sim \left( \frac{2j}{ks} \right) \left( 1 - \frac{j}{ks} \right) G(s), \quad kR \rightarrow \infty \quad (2.8b)$$

When (2.8) is substituted into (2.6a), we find that  $\vec{H}$  in (2.6a) is identical to the *exact* solution of the surface field due to a magnetic dipole on a flat ground plane [4], [13].

The second limiting case occurs when

$$\theta \rightarrow \pi/2 \quad (2.9)$$

We find from (2.6) that  $H_t$  is again given by (2.8b) but  $H_b$  becomes

$$H_b(Q) \sim \left[ 1 - \frac{j}{ks} - \left( \frac{1}{ks} \right)^2 + \frac{3}{4} \left( \frac{\pi}{2} \right)^{1/2} e^{-j\pi/4} \frac{(ks)^{1/2}}{kR} \right] G(s), \quad \theta = \frac{\pi}{2} \quad (2.10a)$$

In terms of the planar solution in (2.8a), we may rewrite (2.10a) as

$$H_b(Q) \sim [H_b(Q)]_{\text{planar}} + \frac{3}{8} \sqrt{\frac{1}{2\pi}} k^2 Y_0 e^{-j3\pi/4} \frac{1}{kR} \frac{e^{-jks}}{\sqrt{ks}}, \quad \theta = \frac{\pi}{2} \quad (2.10b)$$

The result in (2.10) is most interesting, and in fact somewhat surprising. The surface ray traveling in direction  $\theta = \pi/2$  (Fig. 1) is a *straight* line ( $kR_t \rightarrow \infty$ ). However, due to the finite curvature in the binormal direction ( $R_b = R$ ),  $H_b$  on the cylindrical surface differs from its counterpart on a planar surface by the additional term in (2.10b). At a large distance away from the source ( $ks \rightarrow \infty$ ) in the direction  $\theta = \pi/2$ , and for a fixed  $kR$ , we find that  $H_b$  on a planar surface and that on a cylindrical surface are given by, respectively,

$$[H_b(Q)]_{\text{planar}} \sim A \frac{e^{-jks}}{ks} \quad (2.11)$$

$$H_b(Q) \sim B \frac{1}{kR} \frac{e^{-jks}}{\sqrt{ks}} + A \frac{e^{-jks}}{ks}, \quad (2.12)$$

where A and B are constants independent of s and R. Thus, for large ks,  $H_b$  on a cylinder is *stronger* than that on a plane. Such a phenomenon was first reported by Hasserjian and Ishimaru [14], and later by the authors of [4] and [7]. Those previous workers, however, have not explained the phenomenon in terms of  $R_b$ , the radius of curvature in the binomial direction, as we did in (2.6b).

As a third limiting case, let

$$\xi \rightarrow \infty \quad (2.13)$$

which occurs when observation point Q is in the deep shadow. Making use of (A-7) through (A-11), we have from (2.6) that

$$H_b(Q) \sim \frac{k^2 \cos^{2/3} \theta}{1528(kR)^{1/3} (ks)^{1/2}} \exp \left[ -0.88\xi - j \left( \frac{5\pi}{12} + 0.51\xi + ks \right) \right], \quad (2.14a)$$

$$\xi \rightarrow \infty$$

$$H_t(Q) \sim \frac{j}{ks} H_b(Q), \quad \xi \rightarrow \infty \quad (2.14b)$$

Therefore, in the deep shadow, the field is a slow wave and decays exponentially along the surface ray.

In applying the formulas in (2.6) to the mutual admittance calculations [1]-[8], explicit field expressions are needed for axial and circumferential dipoles. They are listed below.

Axial dipole:  $\vec{M} = \hat{z}$  (2.15a)

$$H_z(Q) = H_b \cos^2 \theta + H_t \sin^2 \theta$$

$$\sim \left\{ v(\xi) \left[ \cos^2 \theta - \frac{j}{ks} \cos 2\theta \right] + \left( \frac{j}{ks} \right) u(\xi) \left[ \sin^2 \theta \left( 1 - \frac{2j}{ks} \right) + \left( \frac{j}{ks} \right) \cos^2 \theta \right] \right.$$

$$\left. + j(\sqrt{2} kr_t)^{-2/3} \left[ v'(\xi) \cos^2 \theta + \left( 1 + \frac{j}{ks} \right) u'(\xi) \sin^2 \theta \right] \right\} G(s) \quad (2.15b)$$

Circumferential dipole:  $\vec{M} = \hat{\phi}$  (2.16a)

$$H_\phi(Q) = H_b \sin^2 \theta + H_t \cos^2 \theta$$

$$\sim \left\{ v(\xi) \left[ \sin^2 \theta + \frac{j}{ks} \cos 2\theta \right] + \left( \frac{j}{ks} \right) u(\xi) \left[ \cos^2 \theta \left( 1 - \frac{2j}{ks} \right) + \left( \frac{j}{ks} \right) \sin^2 \theta \right] \right.$$

$$\left. + j(\sqrt{2} kr_t)^{-2/3} \left[ v'(\xi) \sin^2 \theta + \left( \tan^4 \theta + \frac{j}{ks} \right) u'(\xi) \cos^2 \theta \right] \right\} G(s) \quad (2.16b)$$

In the limiting case  $\xi \rightarrow 0$  (either  $kr \rightarrow \infty$  or  $\theta \rightarrow \pi/2$ ), (2.15b) becomes

$$H_z(Q) \sim \left[ \cos^2 \theta + \frac{j}{ks} (2 - 3 \cos^2 \theta) \left( 1 - \frac{j}{ks} \right) \right] G(s), \quad \xi \rightarrow 0 \quad (2.17)$$

and (2.16b) becomes

$$H_\phi(Q) \sim \left[ \sin^2 \theta + \frac{j}{ks} (2 - 3 \sin^2 \theta) \left( 1 - \frac{j}{ks} \right) + W \right] G(s), \quad \xi \rightarrow 0 \quad (2.18a)$$

where

$$W = \begin{cases} 0 & , \text{ if } kr \rightarrow \infty & (2.18b) \\ \frac{3}{4} \left( \frac{j}{2} \right)^{1/2} e^{-j3\pi/4} \frac{(ks)^{1/2}}{kr} & , \text{ if } \theta \rightarrow \pi/2 & (2.18c) \end{cases}$$

Note that in the limit  $kr \rightarrow \infty$ , (2.17) and (2.18) recover the exact solutions for dipoles on a planar surface.

### 3. COMPARISON WITH OSU SOLUTION

For the same problem of a magnetic dipole on a cylinder, an asymptotic (GTD) solution was derived from canonical problems at OSU. That solution, given in Section D of [5] or Eqs. (6.64) and (6.80) of [11], can be also written in the form of (2.6a) with\*

$$H_b(Q) \sim v(\xi)G(s) \quad (3.1a)$$

$$H_t(Q) \sim \left(\frac{j}{ks}\right)u(\xi)G(s) \quad (3.1b)$$

For the extreme case  $\xi \rightarrow 0$  (either  $kR \rightarrow \infty$  or  $\theta \rightarrow \pi/2$ ), the use of (2.7) in (3.1) leads to

$$H_b(Q) \sim G(s), \quad \xi \rightarrow 0 \quad (3.2a)$$

$$H_t(Q) \sim \left(\frac{j}{ks}\right)G(s), \quad \xi \rightarrow 0 \quad (3.2b)$$

For the other extreme case,  $\xi \rightarrow \infty$ , the use of (A-7) and (A-8) in (3.1) leads to an  $H_b$  identical to that in (2.11a), and

$$H_t(Q) \sim \left(\frac{j}{ks}\right) \frac{k^2(ks)^{1/2} \cos^2 \theta}{943(kR)} \exp \left[ -2.03\xi - j \left( \frac{\pi}{4} + 1.17\xi + ks \right) \right], \quad \xi \rightarrow \infty \quad (3.3)$$

The OSU solutions in (3.1), (3.2), and (3.3) should be compared with our solutions in (2.6), (2.8), (2.10) and (2.14). Several remarks are in order.

(1) In the limit  $kR \rightarrow \infty$ , our solution in (2.8) is identical to the known exact solution. On the other hand,  $H_b$  in (3.2a) recovers only the term of  $(ks)^{-1}$ , but not the terms of  $(ks)^{-2}$  or  $(ks)^{-3}$ . The latter terms are important for the field near the source. For  $H_t$  in (3.2b), a factor 2 is missing in the term of  $(ks)^{-2}$ , as pointed out in [5].

\* Note the corresponding notations in [5] and here:  $\psi(\xi) \rightarrow 2e^{-j\pi/4}\xi^{-1/2}v(\xi)$ ,  $\bar{\psi}(\xi) \rightarrow e^{-j3\pi/4}\xi^{-3/2}u(\xi)$ ,  $\alpha \rightarrow \theta$ ,  $a \rightarrow R$ ,  $\rho_g \rightarrow R_t$ , and  $t \rightarrow s$ .

(ii) For a large but finite  $kR$ , the two solutions in (2.6) and (3.1) do not agree. In the penumbra region ( $\xi < 1$ ), the UI solution in (2.6) should be more accurate because of (i). In the deep shadow, both  $H_b$ 's are given by (2.14a), but the two solutions for  $H_t$  in (2.14b) and (3.3) are completely different. In Sections 4 and 6 we will show that (2.14b), not (3.3), agrees with the PINY solution, and gives more accurate numerical results.

(iii) Because of the observations in (i) and (ii), it appears that  $H_t$  given in (3.1b) is not accurate.

(iv) For a fixed  $kR$  and in the direction  $\theta = \pi/2$ ,  $H_b$  in (3.1a) becomes asymptotic for a large  $ks$ ,

$$H_b(Q) \sim A \frac{e^{-jks}}{ks} \quad (3.4)$$

which should be compared with the UI solution in (2.12). We note that the term, attributed to the curvature in the binormal direction of the surface ray, is absent in (3.4).

(v) For acoustic diffraction by a cylinder, the functions  $(v, u)$  arise when the boundary condition is (hard, soft). We note from the OSU solution in (3.1) that  $H_b$  depends on the "hard" function  $v$ , while  $H_t$  depends on the "soft" function  $u$ . Such a separation, however, is not possible for the UI solution in (2.6).

(vi) In Section C of [5], Hwang and Kouyoumjian modified their solution of  $H_t$  in (3.1b) to read

$$\tilde{H}_t(Q) \sim T \left( \frac{j}{ks} \right) u(\xi) G(s) \quad (3.5)$$

Here the additional factor  $T$  for the present cylinder problem is

$$T = \left( \frac{\cos \theta'}{\cos \theta} \right)^4, \quad \text{where } \theta' = \sin^{-1} \left( \frac{\vec{M} \cdot \hat{z}}{|\vec{M}|} \right) \quad (3.6)$$

They attributed the presence of  $T$  to the torsion of the surface ray. However, there exist several apparent difficulties in connection with  $T$ : (a) For a nonaxial dipole ( $\theta' \neq \pi/2$ ),  $T$  becomes infinite as  $\theta \rightarrow \pi/2$ . (b) If  $T$  is indeed a torsion factor, it should be reduced to unity for a torsionless ray propagating in the  $\hat{\phi}$  direction on a cylinder ( $\theta = 0$ ). However,  $T$  calculated from (3.6) does not. (c) An arbitrarily oriented dipole on the surface of a cylinder may be resolved into an axial dipole and a circumferential dipole. We may calculate fields due to each dipole separately, and later superimpose them for the original solution. However, if formulas in (3.5) and (3.1a) are used, such a superposition procedure does not recover the original solution. Because of the above difficulties, we will use (3.1b), not (3.5), for all the subsequent discussion of the OSU solution. (In [3], [4] it is (3.5), not (3.1b), that was used in all the numerical calculations.)

We would like to emphasize that the OSU solution represents one of the very first efforts to apply the ray technique to the surface-field calculation. Their solution, while inadequate in some situations, has produced many useful results [10], [11], and more importantly, has laid a conceptual framework from which the more refined works, e.g., PINY and UI solutions, are deduced.

## 4. COMPARISON WITH PINY SOLUTION

Another asymptotic solution (PINY solution) for the cylinder problem was deduced from the exact modal solution [3], [4], and is given by\*

Axial dipole:  $\vec{M} = \hat{z}$

$$H_z(Q) \sim v(\xi) \left[ \cos^2 \theta + \frac{j}{ks} (2 - 3 \cos^2 \theta) \right] G(s) \quad (4.1)$$

Circumferential dipole:  $\vec{M} = \hat{\phi}$

$$H_\phi(Q) \sim \left\{ v(\xi) \left[ \sin^2 \theta + \frac{j}{ks} (1 - 3 \sin^2 \theta) \right] + \frac{j}{ks} \sec^2 \theta [u(\xi) - \sin^2 \theta v_1(\xi)] \right\} G(s) \quad (4.2)$$

where  $v_1(\xi)$  is defined in the Appendix. In the limiting case  $\xi \rightarrow 0$  (either  $kR \rightarrow \infty$  or  $\theta \rightarrow \pi/2$ ), (4.1) becomes

$$H_z(Q) \sim \left[ \cos^2 \theta + \frac{j}{ks} (2 - 3 \cos^2 \theta) \right] G(s), \quad \xi \rightarrow 0 \quad (4.3)$$

and (4.2) becomes

$$H_\phi(Q) \sim \left[ \sin^2 \theta + \frac{j}{ks} (2 - 3 \sin^2 \theta) + \bar{w} \right] G(s), \quad \xi \rightarrow 0 \quad (4.4a)$$

where

$$\bar{w} = \begin{cases} 0 & , \text{ if } kR \rightarrow \infty \end{cases} \quad (4.4b)$$

$$\bar{w} = \begin{cases} \left(\frac{\pi}{2}\right)^{1/2} e^{-j3\pi/4} \frac{(ks)^{1/2}}{kR} & , \text{ if } \theta \rightarrow \pi/2 \end{cases} \quad (4.4c)$$

The PINY solutions in (4.1) through (4.4) should be compared with the UI solution in (2.15) through (2.18). The following observations are made:

\* There are several slightly different formulas given in [4]. The ones presented here are the "full formulas" taken from Eqs. (101) and (111) of [4]. Note the corresponding notations in [4] and here:  $D \rightarrow s$ ,  $x_s \rightarrow \xi$ ,  $v_0 \rightarrow v$ ,  $v_1 \rightarrow v_1$ , and  $u_0 \rightarrow u$ .

(i) In the limit  $kR \rightarrow \infty$ , the PINY solution recovers the exact solution for a planar surface in terms of  $(ks)^{-1}$  and  $(ks)^{-2}$ , but not in terms of  $(ks)^{-3}$ .

(ii) For a fixed  $kR$  and in the direction  $\theta = \pi/2$ , both  $H_\phi$  of the PINY solution in (4.4) and that of the UI solution in (2.18) vary asymptotically as  $(ks)^{-1/2}$ , which is distinctively different from the  $(ks)^{-1}$  behavior in the planar solution. However, the factor  $W$  in (2.18c) contains an extra factor  $(3/4)$  when compared with its counterpart in (4.4c).

(iii) In the deep shadow  $\xi \rightarrow \infty$ , both  $H_z$  and  $H_\phi$  of the PINY solution decay exponentially according to the "hard" function  $v(\xi)$ , which is in agreement with our solution in (2.11). In particular, at  $\theta = 0$ ,  $H_\phi$  in (4.2) of the PINY solution becomes

$$H_\phi(Q) = H_t(Q) \sim \left(\frac{j}{ks}\right) H_b(Q), \quad \theta = 0 \quad (4.5)$$

where  $H_b(Q)$  is given in (2.14a). Note that (4.5) agrees with the UI solution in (2.14b), but disagrees with the OSU solution in (3.3). It has been demonstrated in [4] (see Figures III-2 and III-13) that the use of (4.5) for mutual admittance calculations between slots shows good agreement with an exact numerical solution, while the result calculated from (3.3) deviates markedly from the exact solution.

(iv)  $H_z$  in (4.1) depends on the "hard" function  $v(\xi)$  only, whereas our solution in (2.15) depends on both  $v(\xi)$  and  $u(\xi)$ .

(v) In Eq. (123) of [4], an expression for  $\vec{H}$  was given for an arbitrarily oriented dipole. It has the form

$$\vec{H}(Q) \sim \vec{M} \cdot [\hat{b}'\hat{b}A + \hat{t}'\hat{t}B + \hat{\phi}'\hat{\phi}C] \quad (4.6)$$

which should be compared with (2.6a). The presence of the cross term  $C$  in (4.6) is unique.

Next, we present a numerical comparison of  $H_\phi$  for all three solutions: the UI solution in (2.16b), the OSU solution in (3.1), and the PINY solution in (4.2). For a cylinder with radius  $kR = 9.5325$ ,  $H_\phi$  on three surface rays ( $\theta = 0^\circ$ ,  $45^\circ$ , and  $90^\circ$ ) is displayed in Figs. 2 to 5 as a function of  $ks$ , the distance from the source. The magnitude of  $H_\phi$  is normalized by  $H_\phi(ks = 0.2, \theta)$  of the UI solution, whereas the normalized phase is equal to  $\text{Arg}(je^{jks} H_\phi)$ . Discussions of these numerical results are given below: (a) As  $ks \rightarrow 0$ , only the UI solution exhibits the correct behavior  $(ks)^{-3}$ . This fact explains the marked disagreement among the three solutions in the range  $0 < ks < 1$ . (b) In the direction  $\theta = 0$  (Fig. 2), UI and PINY solutions converge to each other for  $ks > 6$  (or  $\xi > 1$ ), while the OSU solution is much too small, as noted in (iii) above. (c) In the direction  $\theta = 90^\circ$  in Fig. 5, both the UI and PINY solutions vary as  $(ks)^{-1/2}$ , while the OSU solution varies as  $(ks)^{-1}$ . (d) Overall, the three solutions are significantly different. In applications where accuracy within one or two db is required, the selection of a proper formula becomes crucial.

To present an overall view of the surface magnetic field due to a circumferential dipole ( $\vec{M} = \hat{\phi}$ ), three-dimensional plots of  $|H_\phi|$  and  $|H_z|$  calculated from the UI solution (2.6) are given in Figure 6. Fields in both plots are normalized by  $|H_\phi|$  at  $ks = 0.43$  and  $\theta = \pi/2$ , which has a value 0.00503 a/m and is at zero db. Field values above 7.475 db are not shown in these plots.

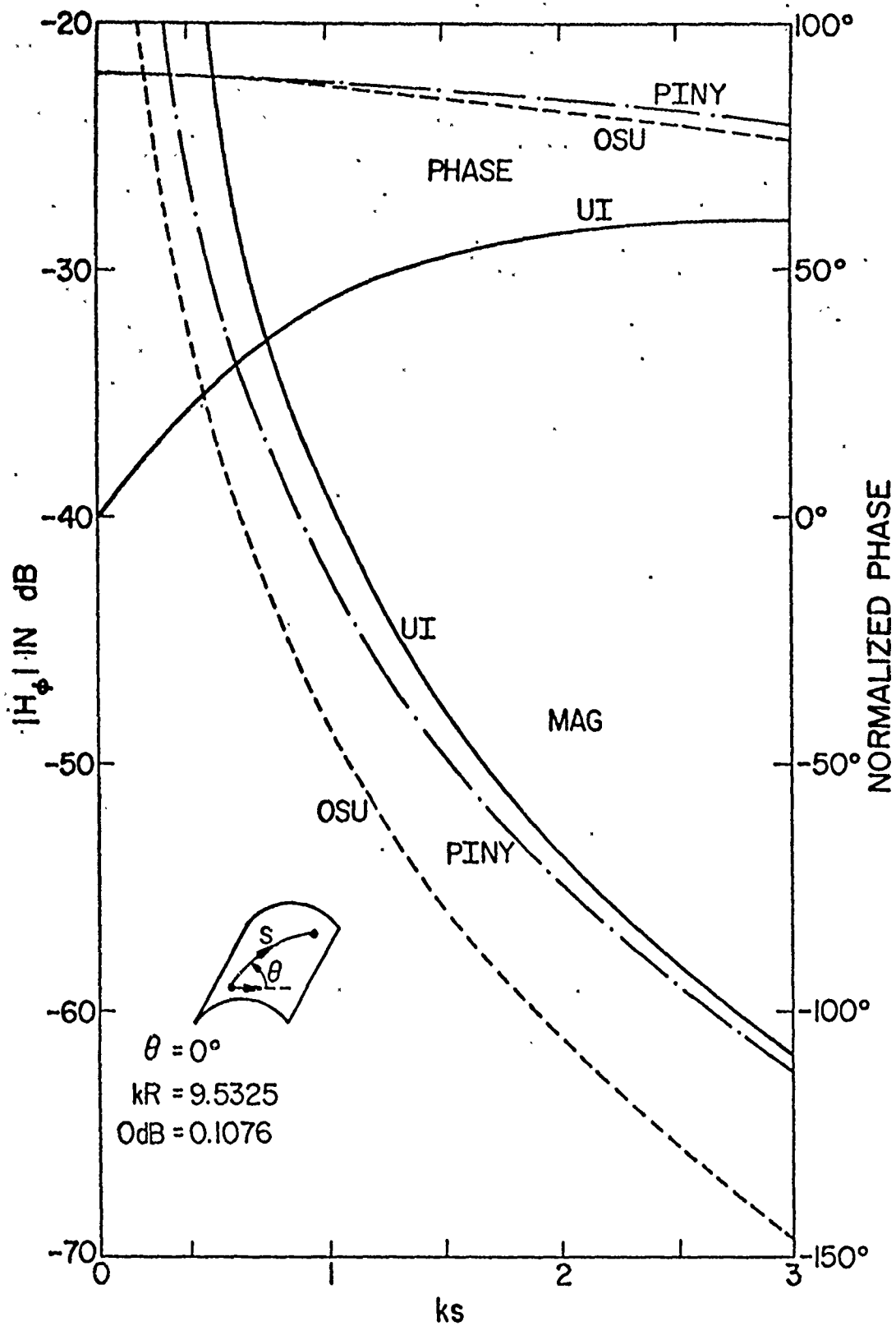


Figure 2.  $H_\phi$  along a surface ray in  $\theta = 0^\circ$  direction on a cylinder vs. the distance from the  $\phi$ -directed magnetic dipole.

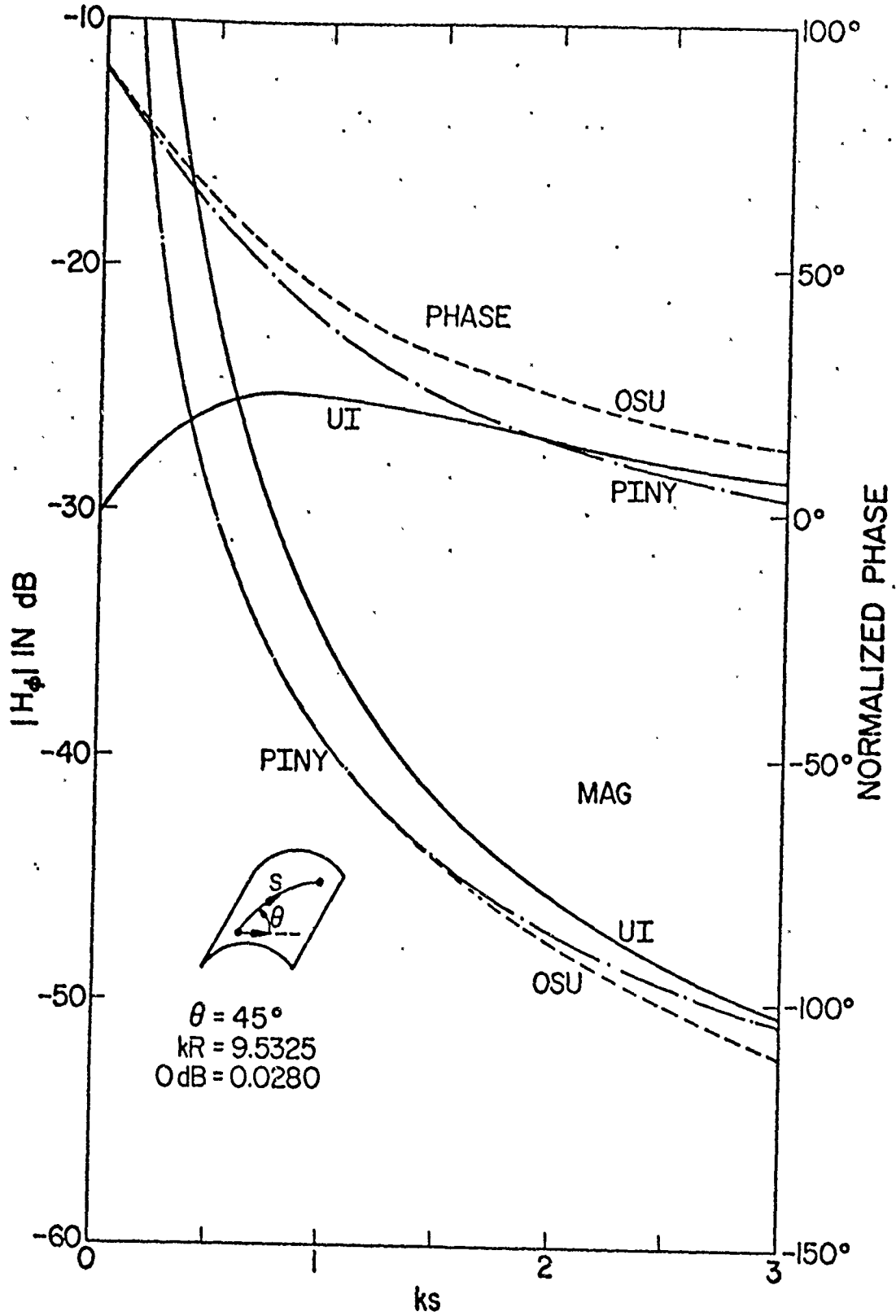


Figure 3.  $H_\phi$  along a surface ray in  $\theta = 45^\circ$  direction on a cylinder vs. the distance from the  $\phi$ -directed magnetic dipole.

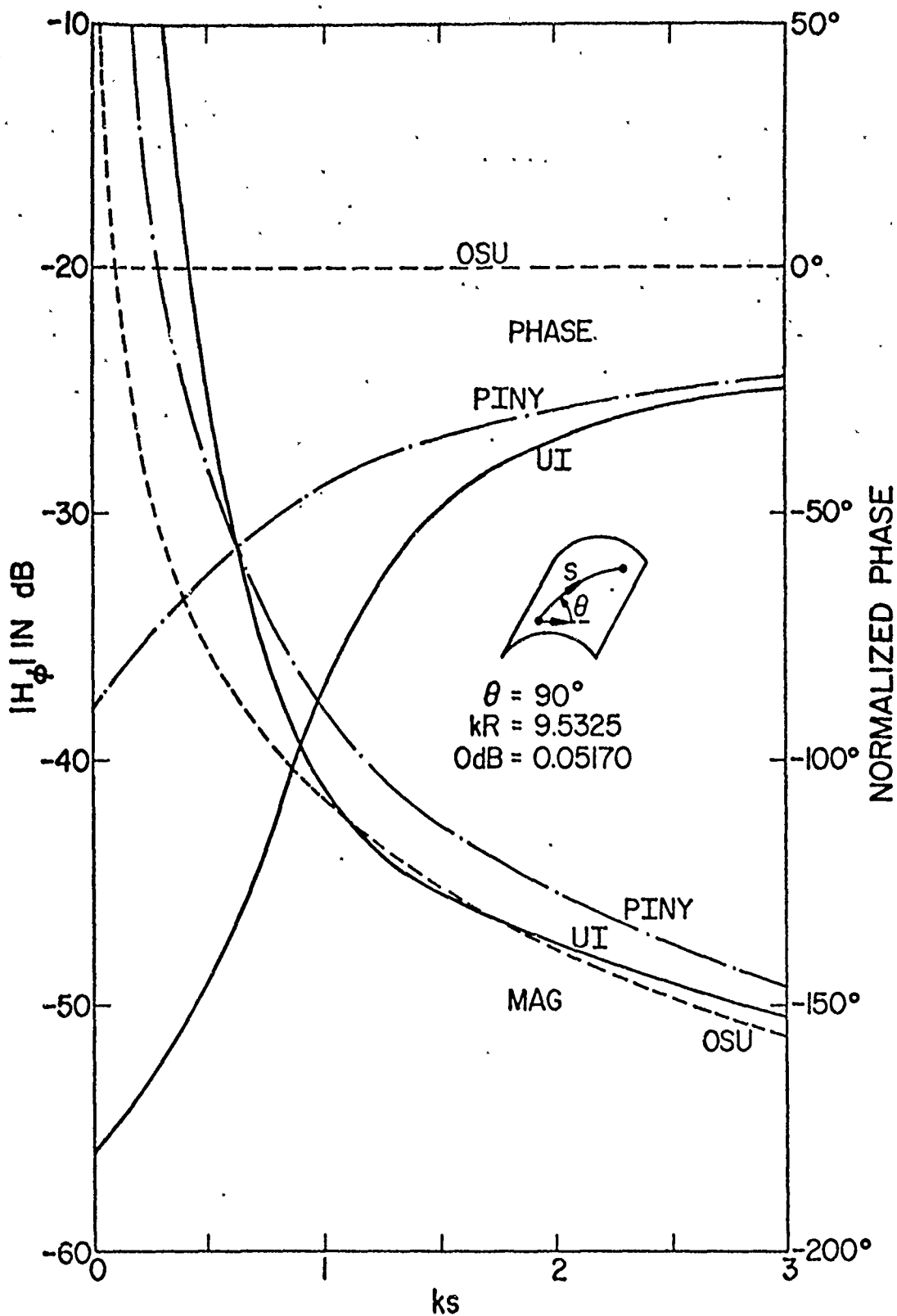


Figure 4.  $H_\phi$  along a surface ray in  $\theta = 90^\circ$  direction on a cylinder vs. the distance from the  $\phi$ -directed magnetic dipole.

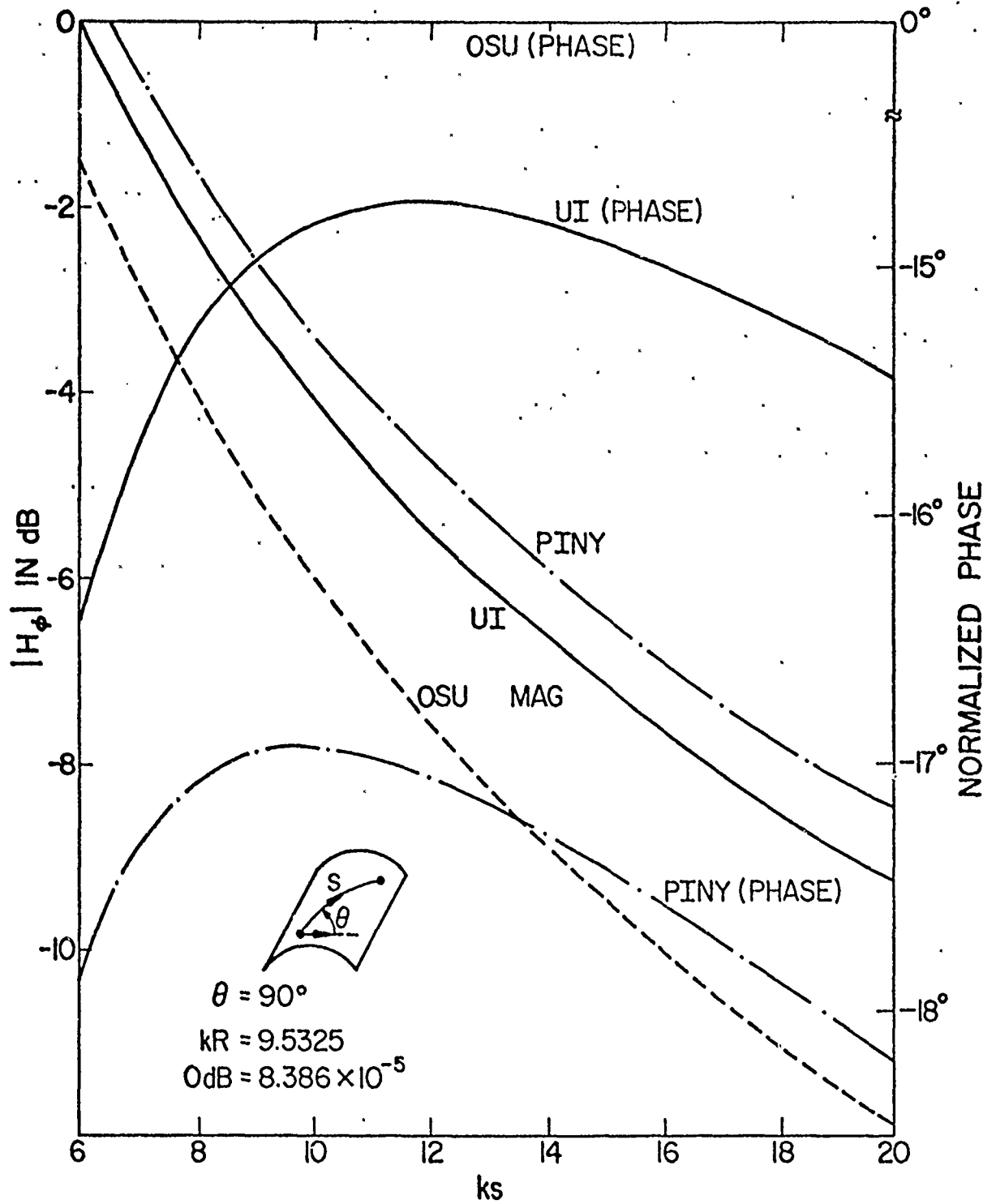


Figure 5.  $H_\phi$  along a surface ray in  $\theta = 90^\circ$  direction on a cylinder vs. the distance from the  $\phi$ -directed magnetic dipole.

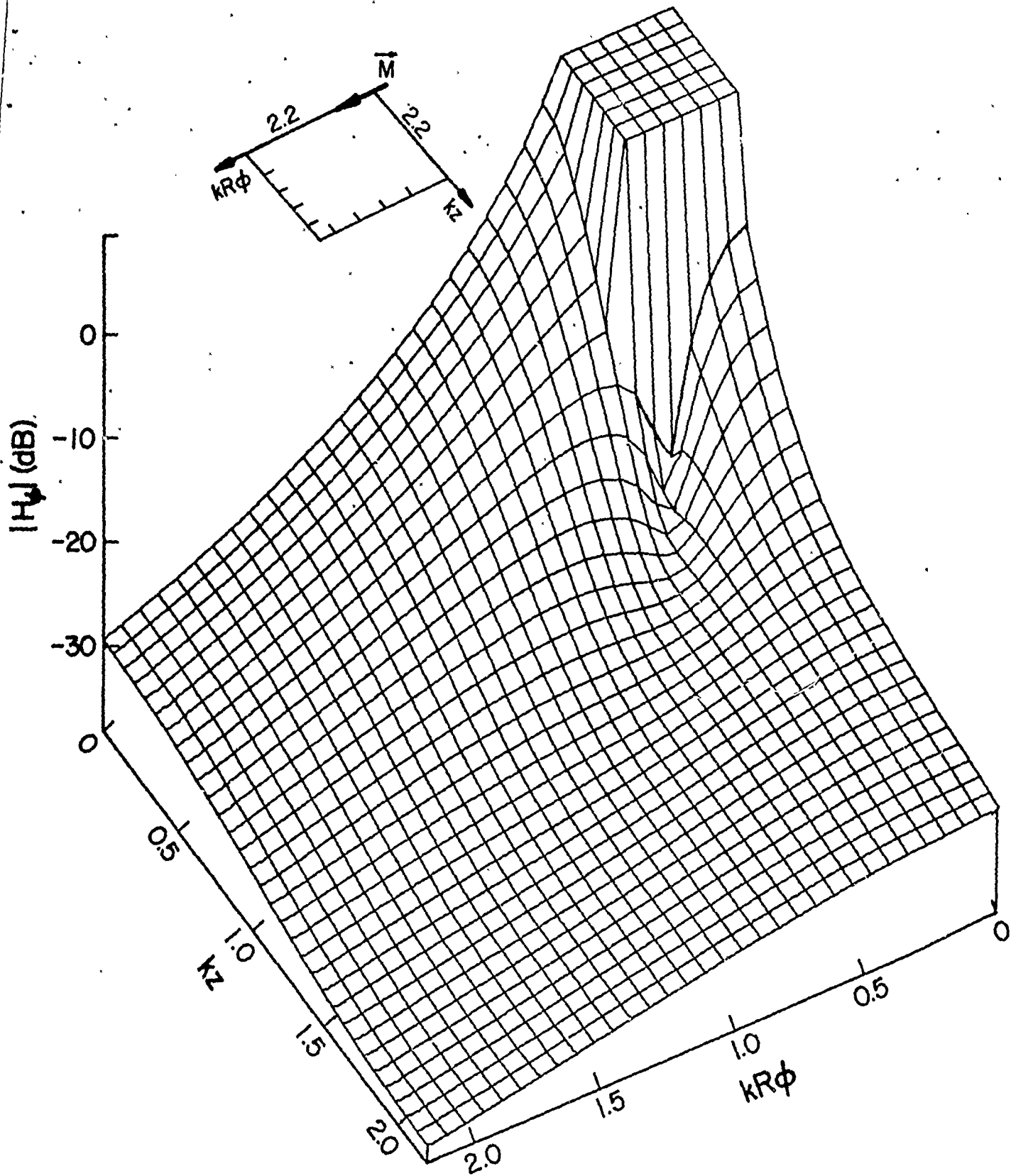
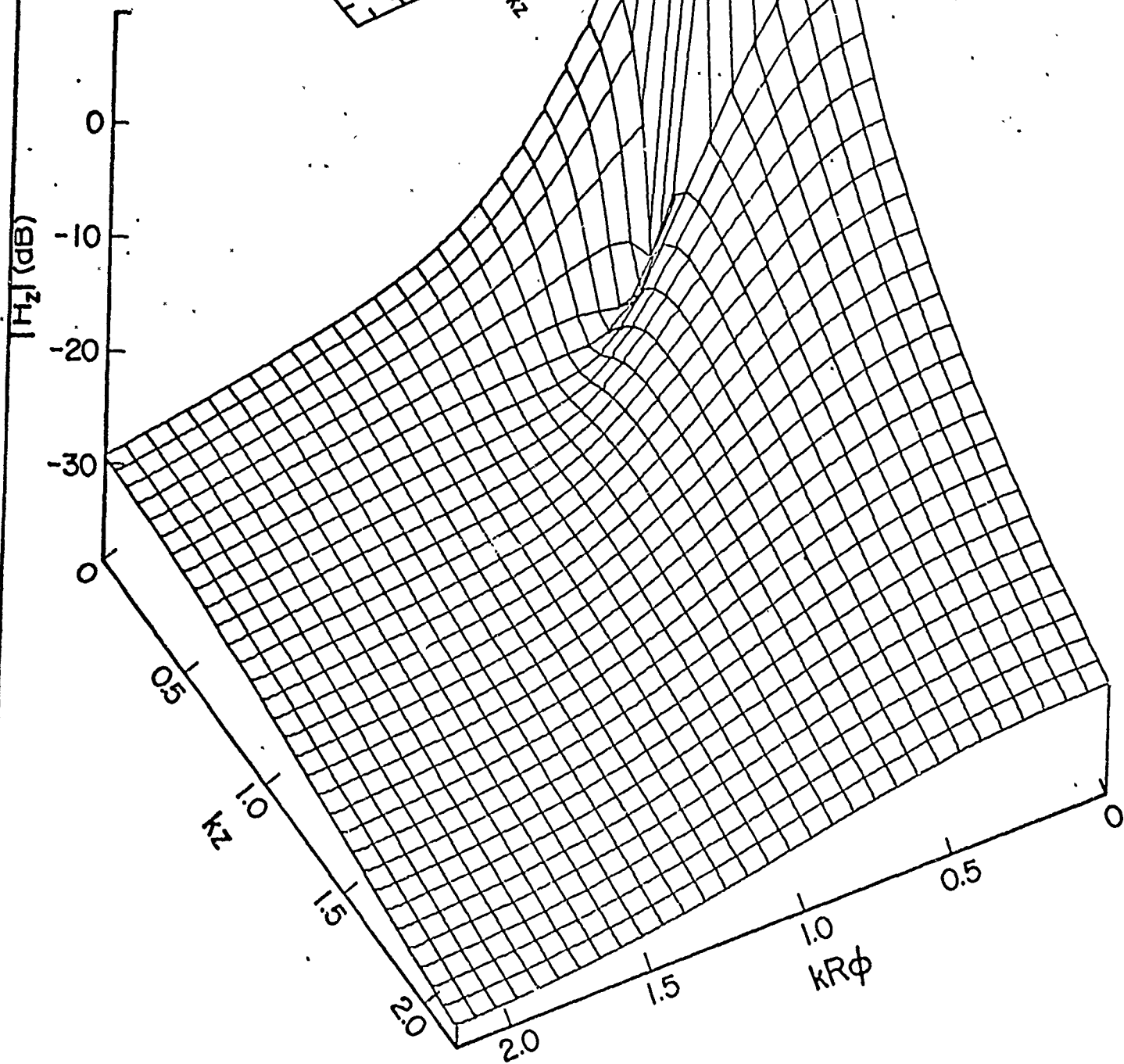
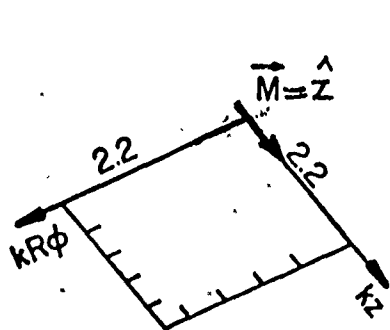


Figure 6. Surface magnetic field  $|H_\phi|$  on a cylinder with  $KR = 9.5125$  due to a circumferential dipole ( $\vec{M} = \hat{\phi}$ ) calculated from (2.6). Values above 7.475 db are not shown.



## 5. APPLICATION: MUTUAL ADMITTANCE OF SLOTS

Let us apply the asymptotic solutions given in the previous three sections to the calculation of the mutual admittance  $Y_{12}$  between two slots on a cylinder. This is done not only because the  $Y_{12}$  calculation is an important practical problem, but also because of the existence of the *exact* modal solution for  $Y_{12}$ , which provides a convenient numerical check of the accuracy of the asymptotic solutions.

Referring to Fig. 7, let us consider two identical circumferential slots on the surface of a cylinder. Under the condition that

$$(a/\lambda) \approx 0.5 \text{ and } (b/\lambda) \ll 1 \quad (5.1)$$

it is reasonable to approximate the aperture field of the slot 1 (or slot 2) by

$$\vec{E}_1(y,z) \approx \hat{z}V_1 \sqrt{\frac{2}{ab}} \cos \frac{\pi}{a} y, \text{ for } |y| < a/2, |z| < b/2 \quad (5.2)$$

where  $y = R\phi$  is the angular distance along the  $\phi$ -direction, and  $V_1$  is the voltage difference across the slot. Once the "one-mode" approximation in (5.2) is accepted, it can be shown [2], [4] that the mutual admittance between the two slots in Fig. 7 is given by

$$Y_{12} = \frac{-2}{ab} \int_{A_1} dy_1 dz_1 \int_{A_2} dy_2 dz_2 \cos \frac{\pi}{a} y_1 \cos \frac{\pi}{a} (y_2 - y_0) g(y_1, z_1; y_2, z_2) \quad (5.3)$$

Here  $A_1$  and  $A_2$  are the apertures of the slots, and  $(y_0, z_0)$  are their center-to-center distances. The Green's function  $g$  in (5.3) represents the  $H_\phi$  at  $(y_2, z_2)$  due to a unit-strength,  $\phi$ -directed magnetic dipole at  $(y_1, z_1)$ . For UI, OSU, and PINY asymptotic solutions of  $Y_{12}$ ,  $g$  is equal to  $H_\phi$  in (2.16b), (3.1), and (4.2), respectively.

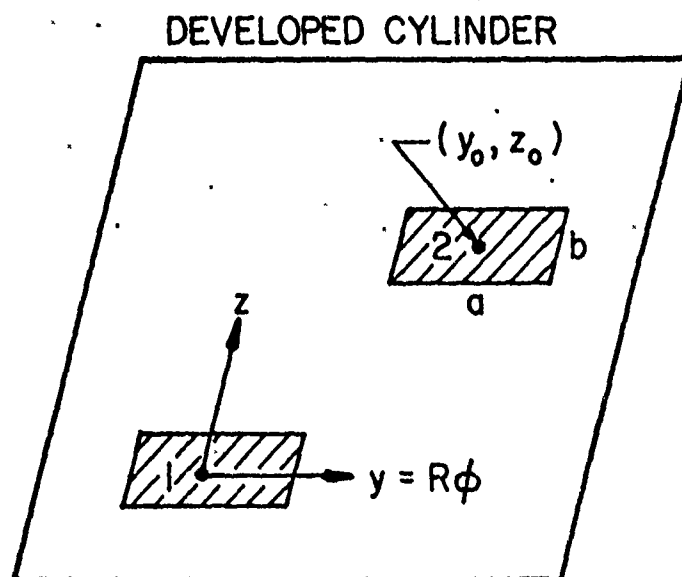


Figure 7. Two identical circumferential slots on the surface of a cylinder. The figure shows the developed cylinder.

In addition to the three asymptotic solutions of  $Y_{12}$ , there exists an expression of  $Y_{12}$  in terms of cylindrical eigenfunctions as given in Eq. (8) of [2].\* Within the "one-mode" approximation, this expression is exact, and contains an infinite series with each term in the series being an infinite integral. This expression has been evaluated by two different numerical techniques. We call the one reported in [2], [7] the Hughes modal solution, and the one in [8] the UI modal solutions.

Now we will present some numerical results calculated from the two (exact) modal solutions, and the three (approximate) asymptotic solutions. The parameters of the cylinder and the slots are

$$f = 9 \text{ GHz}, a = 0.9", b = 0.4", R = 1.991" \quad (5.4)$$

As a function of slot separation  $(z_0, \phi_0)$ ,  $Y_{12}$  is listed in Tables I to III in (db value, phase in degree), where the db value is calculated from the relation

$$\text{db} = 20 \log_{10} |Y_{12}/Y_{11}|, |Y_{11}| = 1.7075 \times 10^{-3} \text{ mho} \quad (5.5)$$

From the comparison made in Tables I to III, we conclude: (a) Considering the numerical integration error involved, the UI asymptotic solution is in excellent agreement with the (exact) modal solution. (b) The PINY asymptotic solution is reasonably accurate, while OSU is not. In addition to the data presented in this paper, we have calculated nearly 100 different  $Y_{12}$ 's over a wide range of parameters. The above two conclusions hold for all the calculations provided that  $kR \geq 5$ .

As discussed in Section 2, the surface ray propagating in the direction  $\theta = \pi/2$  on a cylinder has a stronger  $H_b$  than its counterpart on a plane.

\* There is a misprint in the definition of  $\phi_b$ . The correct one should read  $\phi_b = \sin^{-1}(b/2\rho_0)$ . It should be also pointed out that the corresponding definition used in (5.2) is  $\phi_b = (b/2\rho_0)$ . For numerical data presented in this paper, the two slightly different definitions of  $\phi_b$  have negligible effects.

TABLE I  
 $Y_{12}$  FOR  $\phi_0 = 0$  (E-PLANE)

$z_0$ (inch)	Modal Solutions		Asymptotic Solutions			Planar $R = \infty$
	Hughes	UI	UI	OSU	PINY	
0.5"	-7.27 db	-7.27	-7.19	-8.87	-6.35	-8.04
	$-72^\circ$	$-72^\circ$	$-72^\circ$	$-43^\circ$	$-68^\circ$	$-67^\circ$
2"	-16.52	-16.43	-16.31	-18.32	-15.61	-18.18
	$-117^\circ$	$-117^\circ$	$-116^\circ$	$-100^\circ$	$-118^\circ$	$-106^\circ$
8"	-26.95	-26.49	-26.48	-30.11	-25.45	-30.05
	$33^\circ$	$34^\circ$	$37^\circ$	$55^\circ$	$34^\circ$	$54^\circ$
16"		-31.13	-31.25	-36.06	-29.91	-36.05
		$-4^\circ$	$-1^\circ$	$20^\circ$	$-4^\circ$	$19^\circ$
40"		-36.60	-37.11	-43.99	-35.48	-43.98
		$-115^\circ$	$-110^\circ$	$-83^\circ$	$-112^\circ$	$-83^\circ$

TABLE II

 $Y_{12}$  FOR  $z_0 = 2''$ 

$\phi_0$ (deg)	Modal Solutions		Asymptotic Solutions		
	Hughes	UI	UI	OSU	PINY
$0^\circ$	-16.52 db	-16.43	-16.31	-18.32	-15.61
	$-117^\circ$	$-117^\circ$	$-116^\circ$	$-100^\circ$	$-118^\circ$
$30^\circ$	-22.25	-22.07	-22.34	-23.90	-21.25
	$175^\circ$	$175^\circ$	$177^\circ$	$-170^\circ$	$172^\circ$
$60^\circ$	-34.63	-34.65	-34.82	-35.76	-33.06
	$-4^\circ$	$-3^\circ$	$-1^\circ$	$6^\circ$	$-10^\circ$
$90^\circ$	-47.82	-47.17	-47.75	-48.48	-46.34
	$116^\circ$	$120^\circ$	$116^\circ$	$119^\circ$	$106^\circ$

TABLE III

 $Y_{12}$  FOR  $z_0 = 0$  (H-PLANE)

$\phi_0$ (deg)	Modal	Asymptotic Solutions		
	Hughes	UI	OSU	PINY
$30^\circ$	-25.98 db	-25.99	-34.37	-27.79
	$-77^\circ$	$-75^\circ$	$-62^\circ$	$-60^\circ$
$40^\circ$	-34.52	-34.67	-43.31	-35.76
	$168^\circ$	$170^\circ$	$174^\circ$	$-180^\circ$
$50^\circ$	-40.96	-41.37	-50.60	-42.08
	$58^\circ$	$61^\circ$	$58^\circ$	$69^\circ$
$60^\circ$	-46.62	-47.13	-57.24	-47.58
	$-49^\circ$	$-47^\circ$	$-55^\circ$	$-39^\circ$

Since  $Y_{12}$  along the E-plane ( $\phi_0 = 0$ ) is proportional to  $H_b$ , this phenomenon is also seen in Figure 8, where we plot the ratio

$$\left| \frac{Y_{12} \text{ on a cylinder with radius } R}{Y_{12} \text{ on a plane}} \right|$$

as a function of  $R$  for  $z_0 = 8''$  and  $\phi_0 = 0$ . We note that the convergence rate of the cylindrical  $Y_{12}$  to the planar  $Y_{12}$  is not as rapid as one would normally expect. For example, at  $kR = 50$ , the cylindrical  $Y_{12}$  is still about 10 percent higher than the planar one.

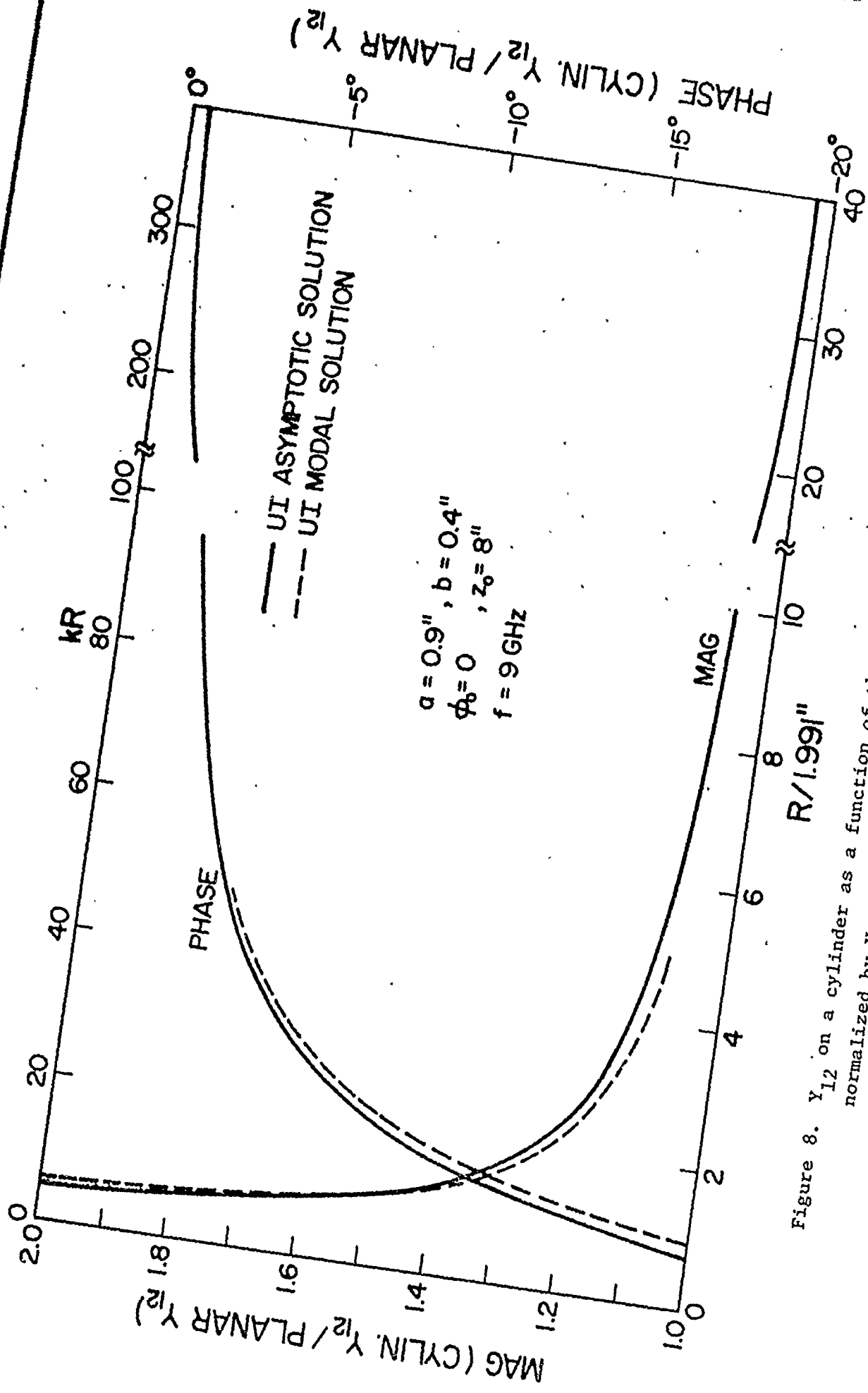


Figure 8.  $Y_{12}$  on a cylinder as a function of the radius  $R$  of the cylinder.  $Y_{12}$  is normalized by  $Y_{12}$  on a plane which is  $5.37 \times 10^{-5} \exp(j53.55^\circ)$  mho.

## 6. DERIVATION OF UI SOLUTION

The UI solution given in (2.6) will now be derived. The derivation is based on the following observation. Consider a surface ray (a geodesic) on an arbitrary convex surface. In the neighborhood of the ray, the geometrical properties of the surface depend on two radii of curvature:  $R_t$  in the direction of tangent  $\hat{t}$  and  $R_b$  in the direction of binormal  $\hat{b}$ . It is well-known that the *dominant* asymptotic solution of a surface field depends on  $R_t$ , not  $R_b$  (see the discussion in pp. 192-193 of [11]). Thus, for the purpose of determining the dominant term of the surface field in the direction of  $\theta$  in Fig. 1, the cylinder may be replaced by, for example, a sphere of radius  $R_t$ . In other words, our problem is then to solve the radiation of a magnetic dipole on a perfectly conducting sphere.

In studying wave propagation around the earth in 1949, Fock considered the radiation of a horizontal electric dipole on a lossy dielectric sphere [12]. He first obtained an exact solution in terms of spherical harmonics, and next extracted the dominant high-frequency terms from it. By the duality principle, Fock's solution can be converted to the one that is sought by us. We will give below the solution after the conversion is done.

Consider a magnetic dipole in the x-direction ( $\vec{M} = \hat{x}$ ), located on a perfectly conducting sphere of radius  $R_t$  (Fig. 9). The total field can be derived from a magnetic Hertz potential  $U$  and an electric Hertz potential  $V$ . The asymptotic solutions of  $U$  and  $V$  are found to be [from (7.09) and (7.10) on p. 252 of [12]]\*

\* The divergence factor  $DF$  of the surface ray on a sphere has been removed in (6.1) [ $DF = (\theta/\sin \theta)^{1/2}$ ]. Note the corresponding notations in [12] and here:  $i \rightarrow (-j)$ ,  $u \rightarrow U$ ,  $v \rightarrow V$ ,  $a \rightarrow R_t$ , and  $x \rightarrow \xi$ .

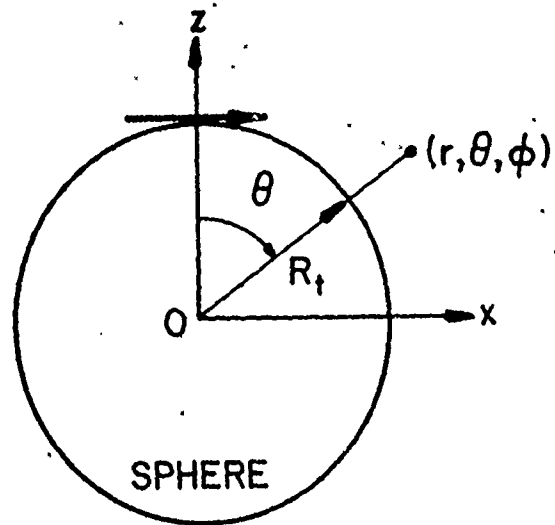


Figure 9. A horizontal magnetic dipole on the surface of a perfectly conducting sphere.

$$U(\vec{r}) \sim G(s) \frac{\cos \phi}{2k^2 R_t m} e^{-j\pi/4} (\xi/\pi)^{1/2} \int_{\Gamma_1} e^{-j\xi t} \left[ \frac{j}{2} w_2'(t) \left[ w_1(t - y_1) - \frac{w_1(t)}{w_2(t)} w_2(t - y_1) \right] \right] dt \quad (6.1a)$$

$$\left[ V(r) \right]_{r=R_t} \sim G(s) \frac{-\sin \phi}{k^2 R_t} v(\xi) \quad (6.1b)$$

where  $y_1 = (k/m)(r - R_t)$ , and  $(r, \theta, \phi)$  are the spherical coordinates of  $\vec{r}$ . Parameters  $G$ ,  $m$ , and  $\xi$  in (6.1) are defined in Section 2, while the others are in the Appendix. The magnetic field is calculated from the relations

$$H_r(\vec{r}) = \left[ \frac{1}{r \sin \theta} \frac{\partial}{\partial \theta} \left( \sin \theta \frac{\partial}{\partial \theta} \right) + \frac{1}{r \sin^2 \theta} \frac{\partial^2}{\partial \phi^2} \right] U \quad (6.2a)$$

$$H_\theta(\vec{r}) = -\frac{1}{r} \frac{\partial^2}{\partial r \partial \theta} (rU) + \frac{k}{j \sin \theta} \frac{\partial}{\partial \phi} V \quad (6.2b)$$

$$H_\phi(\vec{r}) = -\frac{1}{r \sin \theta} \frac{\partial^2}{\partial r \partial \phi} (rU) + jk \frac{\partial}{\partial \theta} V \quad (6.2c)$$

Substituting (6.2) into (6.1) and using the results

$$\frac{\partial}{\partial r} = \frac{k}{m} \frac{\partial}{\partial y_1}, \quad \frac{\partial}{\partial \theta} = R_t \frac{\partial}{\partial s} = m \frac{\partial}{\partial \xi} \quad (6.3a)$$

$$\left[ \frac{\partial}{\partial r} (rU) \right]_{r=R_t} = \frac{\cos \phi}{k^2 s} G(s) u(\xi) \quad (6.3b)$$

we obtain the magnetic field on the surface, namely,

$$H_r(R_t, \theta, \phi) \sim 0 \quad (6.4a)$$

$$H_\theta(R_t, \theta, \phi) \sim \cos \phi \left[ \frac{j}{ks} \right] \left[ v(\xi) + \left( 1 - \frac{2j}{ks} \right) u(\xi) + \frac{jm}{kR_t} u'(\xi) \right] G(s) \quad (6.4b)$$

$$H_\phi(R_t, \theta, \phi) \sim -\sin \phi \left[ \left(1 - \frac{j}{ks}\right) v(\xi) - \left(\frac{1}{ks}\right)^2 u(\xi) + M \right] G(s) \quad (6.4c)$$

where

$$M = \frac{j\mathfrak{m}}{kR_t} v'(\xi) \quad (6.5)$$

From the derivation of U and V in (6.1) it may be shown that (6.4) is asymptotically accurate only up to and including terms of order  $(kR_t)^{-2/3}$ . Thus, the last terms in (6.4b) and (6.4c), which are of order  $(kR_t)^{-1}$ , may or may not be completed. We hereby modify the factor M in (6.5) to read

$$\dot{M} = \frac{j\mathfrak{m}}{kR_t} \left[ v'(\xi) + \frac{R_t}{R_b} u'(\xi) \right] \quad (6.6)$$

The only "justification" for replacing (6.5) by (6.6) is that this replacement yields no appreciable difference in the sphere problem (where  $R_t/R_b = 1$ ), but significantly improves the numerical solution for the cylinder problem (where  $R_t/R_b$  may be very large) as shown in Section 5. We have not yet succeeded in finding a rigorous justification for using (6.6). Referring to the cylinder geometry sketched in Fig. 1, the following substitutions are made

$$H_r \rightarrow H_n, \quad (H_\theta/\cos \phi) \rightarrow H_t, \quad (H_\phi/\sin \phi) \rightarrow -H_b, \quad \phi \rightarrow \theta \quad (6.7)$$

Then (6.4) and (6.6) become identical to (2.6).

It should be mentioned that expressions similar to (6.4) were given by Wait in 1956 [15], and by Hasserjian and Ishimaru in 1962 [14], [16]. Their expressions contain only  $(ks)^{-1}$  terms, and therefore only the "hard" function  $v(\xi)$  is used.

## 7. CONCLUSION

For a given magnetic dipole located on a perfectly conducting cylinder, the surface magnetic field is given in (2.6), which is an approximate asymptotic solution valid for large  $kR$ , and may be used for any observation point on the cylinder. The derivation of (2.6) is based on the following observation: the dominant contribution of the surface field depends on the curvature of the surface in the longitudinal direction of the ray, not that in the transverse direction. Hence, we simply adopt the classical solution of Fock for a dipole on a sphere for the present cylinder problem. To include the effect of the curvature in the binormal direction of the surface ray, we have arbitrarily replaced a factor  $M$  of the Fock solution in (6.5) by that in (6.6). A rigorous justification of this replacement is yet to be found. A remarkable feature of the solution in (2.6) is that in the limit  $kR \rightarrow \infty$ , it becomes identical to the known exact solution of a dipole on a flat ground plane. The application of (2.6) to the mutual admittance calculation yields excellent numerical results, and therefore (2.6) may be regarded as an improvement over two previous asymptotic solutions. A future research problem is to generalize (2.6), according to the recipe of GTD, so that it may be used for an arbitrary convex conducting surface.

## APPENDIX

## FOCK FUNCTIONS

In this appendix we define and list some useful formulas of the functions  $w_1(t)$ ,  $w_2(t)$ ,  $v(\xi)$ ,  $u(\xi)$ , and  $v_1(\xi)$ . These functions are commonly known as Fock functions.

(i) Definition: For a complex  $t$  and a real  $\xi$ ,

$$w_1(t) = \frac{1}{\sqrt{\pi}} \int_{\Gamma_1} dz \exp \left( tz - \frac{1}{3} z^3 \right) \quad (\text{A-1})$$

$$w_2(t) = \frac{1}{\sqrt{\pi}} \int_{\Gamma_2} dz \exp \left( tz - \frac{1}{3} z^3 \right) = w_1^*(t) \quad (\text{A-2})$$

$$v(\xi) = \frac{1}{2} e^{j\pi/4} \xi^{1/2} \frac{1}{\sqrt{\pi}} \int_{\Gamma_1} \frac{w_2(t)}{w_2'(t)} e^{-j\xi t} dt \quad (\text{A-3})$$

$$u(\xi) = e^{j3\pi/4} \xi^{3/2} \frac{1}{\sqrt{\pi}} \int_{\Gamma_1} \frac{w_2'(t)}{w_2(t)} e^{-j\xi t} dt \quad (\text{A-4})$$

$$v_1(\xi) = e^{j3\pi/4} \xi^{3/2} \frac{1}{\sqrt{\pi}} \int_{\Gamma_1} t \frac{w_2(t)}{w_2'(t)} e^{-j\xi t} dt \quad (\text{A-5})$$

where integration contours  $\Gamma_1$  and  $\Gamma_2$  are sketched in Figure 10, and  $w_2'(t)$  is the derivative of  $w_2(t)$ .

(ii) Zeros of  $w_2(t)$  and  $w_2'(t)$ : They are given by

$$t = t_n = |t_n| e^{-j\pi/3}, \text{ and } t = t'_n = |t'_n| e^{-j\pi/3}, \quad (\text{A-6})$$

respectively. The magnitudes of the first ten zeros are

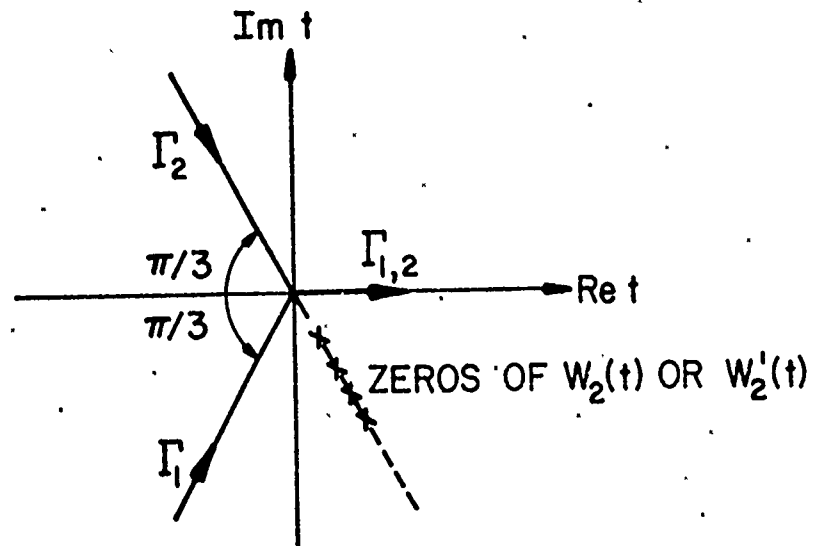


Figure 10. Contours  $\Gamma_1$  and  $\Gamma_2$  on the complex  $t$  (or  $z$ ) plane.  $\Gamma_1$ , for example, goes from  $\infty$  to 0 along the line  $\text{Arg } t = -2\pi/3$  and from 0 to  $\infty$  along the real axis.

n	$ t_n $	$ t'_n $
1	2.33811	1.01879
2	4.08795	3.24820
3	5.52056	4.82010
4	6.78671	6.16331
5	7.99417	7.37218

n	$ t_n $	$ t'_n $
6	5.02265	8.48849
7	10.04017	9.53545
8	11.00852	10.52766
9	11.93602	11.47506
10	12.82878	12.38479

(iii) Residue series representation: For real positive  $\xi$ ,

$$v(\xi) = e^{-j\pi/4} \sqrt{\pi} \xi^{1/2} \sum_{n=1}^{\infty} (t'_n)^{-1} e^{-j\xi t'_n} \quad (\text{A-7})$$

$$u(\xi) = e^{j\pi/4} 2\sqrt{\pi} \xi^{3/2} \sum_{n=1}^{\infty} e^{-j\xi t_n} \quad (\text{A-8})$$

$$v_1(\xi) = e^{j\pi/4} 2\sqrt{\pi} \xi^{3/2} \sum_{n=1}^{\infty} e^{-j\xi t'_n} \quad (\text{A-9})$$

$$v'(\xi) = \frac{1}{2} e^{-j\pi/4} \sqrt{\pi} \xi^{-1/2} \sum_{n=1}^{\infty} (1 - j2\xi t'_n) (t'_n)^{-1} e^{-j\xi t'_n} \quad (\text{A-10})$$

$$u'(\xi) = e^{j\pi/4} 3\sqrt{\pi} \xi^{1/2} \sum_{n=1}^{\infty} \left(1 - j \frac{2}{3} \xi t_n\right) e^{-j\xi t_n} \quad (\text{A-11})$$

(iv) Small argument asymptotic expansion: For real positive  $\xi$  and  $\xi \rightarrow 0$ ,

$$v(\xi) \sim 1 - \frac{\sqrt{\pi}}{4} e^{j\pi/4} \xi^{3/2} + \frac{7j}{60} \xi^3 + \frac{7\sqrt{\pi}}{512} e^{-j\pi/4} \xi^{9/2} - 4.141 \times 10^{-3} \xi^6 + \dots \quad (\text{A-12})$$

$$u(\xi) \sim 1 - \frac{\sqrt{\pi}}{2} e^{j\pi/4} \xi^{3/2} + \frac{5j}{12} \xi^3 + \frac{5\sqrt{\pi}}{64} e^{-j\pi/4} \xi^{9/2} - 3.701 \times 10^{-2} \xi^6 + \dots \quad (\text{A-13})$$

$$v_1(\xi) \sim 1 + \frac{\sqrt{\pi}}{2} e^{j\pi/4} \xi^{3/2} - \frac{7j}{12} \xi^3 - \frac{7\sqrt{\pi}}{64} e^{-j\pi/4} \xi^{9/2} + 4.555 \times 10^{-2} \xi^6 + \dots \quad (\text{A-14})$$

$$v'(\xi) \sim \frac{3\sqrt{\pi}}{8} e^{-j3\pi/4} \xi^{1/2} + \frac{7j}{20} \xi^2 + \frac{63\sqrt{\pi}}{1024} e^{-j\pi/4} \xi^{7/2} - 2.485 \times 10^{-2} \xi^5 + \dots \quad (\text{A-15})$$

$$u'(\xi) \sim \frac{3}{4} \sqrt{\pi} e^{-j3\pi/4} \xi^{1/2} + \frac{5j}{4} \xi^2 + \frac{45\sqrt{\pi}}{128} e^{-j\pi/4} \xi^{7/2} - 2.221 \times 10^{-1} \xi^5 + \dots \quad (\text{A-16})$$

(v) Relation to Fock's attenuation factor: The attenuation factor  $V(x, y, q)$  is defined by Fock in p. 207 of [12], and it reads (after replacing  $i$  by  $-j$ )

$$V(x, y, q) = e^{j\pi/4} x^{1/2} \frac{1}{\sqrt{\pi}} \int_{\Gamma_1} \frac{w_2(t-y)}{w_2'(t) - qw_2(t)} e^{-jxt} dt \quad (\text{A-17})$$

The functions  $v$  and  $u$  are related to  $V$  by

$$v(x) = \frac{1}{2} V(x, y=0, q=0) \quad (\text{A-18})$$

$$u(x) = jx \lim_{q \rightarrow \infty} q \left[ \frac{\partial V}{\partial y} \right]_{y=0} \quad (\text{A-19})$$

(vi) Relation to functions defined by Logan [17]:

$$v(\xi) = \frac{1}{2} e^{+j\pi/4} \xi^{1/2} \psi(\xi) \quad (\text{A-20})$$

$$u(\xi) = e^{j3\pi/4} \xi^{3/2} \bar{\psi}(\xi) \quad (\text{A-21})$$

(vii) Tabulation: Functions  $w_1(t)$ ,  $w_2(t)$  and their derivatives are tabulated in [12], while  $\psi(\xi)$  and  $\bar{\psi}(\xi)$  are tabulated in [17]. Numerical curves of  $u$ ,  $v$ , and  $v_1$  can be found in [4], [14], [15].

(viii) Numerical evaluation: For  $\xi \geq \xi_0$ , the residue series representation with the first ten terms in the summation may be used. For  $\xi \leq \xi_0$ , the small argument asymptotic expansion with the first five terms may be used. It has been indicated in [4] that the smoothest crossover is obtained if  $\xi_0 = 0.6$ . In the present study, we set  $\xi_0 = 0.7$ , where the difference in the two representations is as follows.

Difference at $\xi = 0.7$		
	Mag. (%) <sup>*</sup>	Phase (deg.)
v	0.00	0.00
u	0.11	0.01
v <sub>1</sub>	0.02	0.08
v'	0.09	0.15
u'	0.10	0.90

$$*\% = |1 - (\text{Residue/Small arg.})| \times 100$$

## REFERENCES

- [1] G. E. Stewart and K. E. Golden, "Mutual admittance for axial rectangular slots in a large conducting cylinder," IEEE Trans. Antennas Propagat., vol. AP-19, pp. 120-122, 1971.
- [2] K. E. Golden, G. E. Stewart, and D. C. Pridmore-Brown, "Approximation techniques for the mutual admittance of slot antennas on metallic cones," IEEE Trans. Antennas Propagat., vol. AP-22, pp. 43-48, 1974.
- [3] Z. W. Chang, L. B. Felsen, A. Hessel and J. Shmoys, "Surface ray method in the analysis of conformal arrays," Digest of 1976 AP-S International Symposium, held at University of Massachusetts at Amherst, October 1976, pp. 366-369.
- [4] Z. W. Chang, L. B. Felsen, and A. Hessel, "Surface ray methods for mutual coupling in conformal arrays on cylinder and conical surface," Polytechnic Institute of New York, Final Report (September 1975-February 1976), prepared under Contract N00123-76-C-0236, 1976.
- [5] Y. Hwang and R. G. Kouyoumjian, "The mutual coupling between slots on an arbitrary convex cylinder," ElectroScience Laboratory, Department of Electrical Engineering, The Ohio State University, Semi-Annual Report 2902-21, prepared under Grant NGL 36-003-138, 1975.
- [6] P. H. Pathak, "Analysis of a conformal receiving array of slots in a perfectly-conducting circular cylinder by the geometrical theory of diffraction," ElectroScience Laboratory, Department of Electrical Engineering, The Ohio State University, Technical Report ESL 3735-2, prepared under Contract N00140-74-C-6017, 1975.
- [7] P. C. Bargeliotis, A. T. Villeneuve, and W. H. Kummer, "Phased array antennas scanned near endfire," Final Report (January 1975-March 1976), Contract N00019-75-0160, Hughes Aircraft Company, Culver City, California, 1976.
- [8] S. Safavi-Naini and S. W. Lee, "Calculation of mutual admittance between slots on a cylinder," to be published.
- [9] J. B. Keller, "Geometrical theory of diffraction," J. Opt. Soc. Amer., vol. 52, pp. 116-130, 1962.
- [10] P. H. Pathak and R. G. Kouyoumjian, "An analysis of the radiation from apertures in curved surfaces by the geometric theory of diffraction," Proc. IEEE, vol. 62, pp. 1438-1461, November 1974.
- [11] R. G. Kouyoumjian, "The geometrical theory of diffraction and its application," in Topics in Applied Physics, R. Mittra, Ed. New York: Springer-Verlag, 1975.
- [12] V. A. Fock, Electromagnetic Diffraction and Propagation Problems. New York: Pergamon Press, 1965.

- [13] L. B. Felsen and N. Marcuvitz, Radiation and Scattering of Waves. Englewood Cliffs, New Jersey: Prentice-Hall, 1973, pp. 477 and 483.
- [14] G. Hasserjian and A. Ishimaru, "Current induced on the surface of a conducting circular cylinder by a slot," J. Res. Nat. Bur. Stand., D. Radio Propagation, vol. 66, pp. 335-365, 1962.
- [15] J. R. Wait, "Currents excited on a conducting surface of large radius of curvature," IRE Trans., vol. MTT-4, no. 3, pp. 143-145, 1956.
- [16] G. Hasserjian and A. Ishimaru, "Excitation of a conducting cylindrical surface of large radius of curvature," IRE Trans., vol. AP-10, pp. 264-273, 1962.
- [17] N. A. Logan, "General research in diffraction theory," Missiles and Space Div., Lockheed Aircraft Corp., vol. 1, Rept. LMSD-288087 and vol. 2, Rept. LMSD-288088, December 1959.